

KATRIN Experiment

Direct neutrino-mass measurement with sub-electronvolt sensitivity

Group C



Motivation

- From neutrino oscillations:
non-zero m_ν
- **Hierarchy of masses** is open
- Can be associate to **Cosmology**
- **Precision is needed!**
- **Anything** can be a **background**
- **Huge engineering** achievement

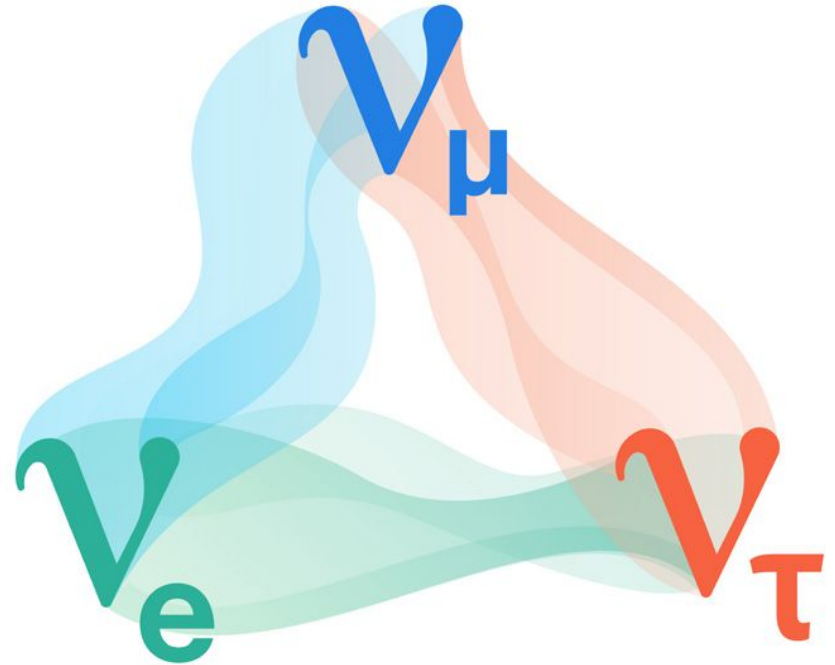


The Effective Mass

NOTE: KATRIN measures an **effective mass** for the ν_e

$$m_{\nu}^2 = \sum_i |U_{ei}|^2 m_i^2$$

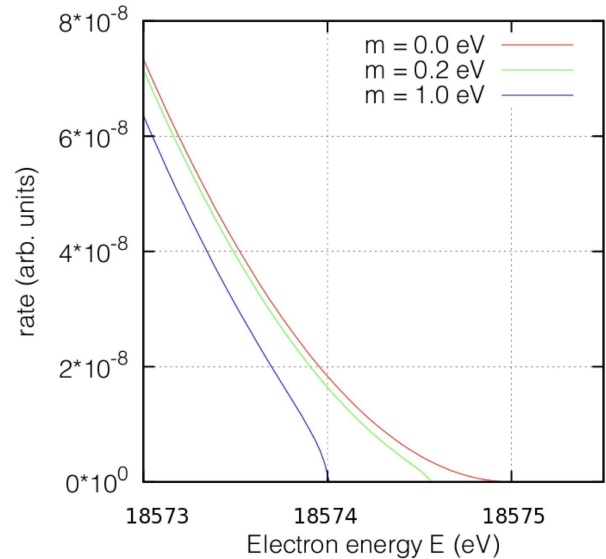
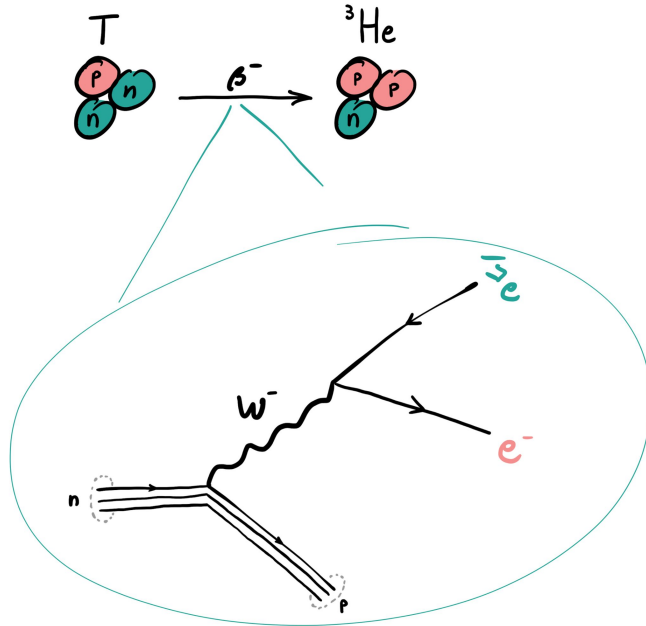
*Under the assumption that the **mass scale is larger than the mass splittings**



How can
KATRIN
experiment
measure m_ν
precisely?



We can produce ν_e through the β^- decay, and ...



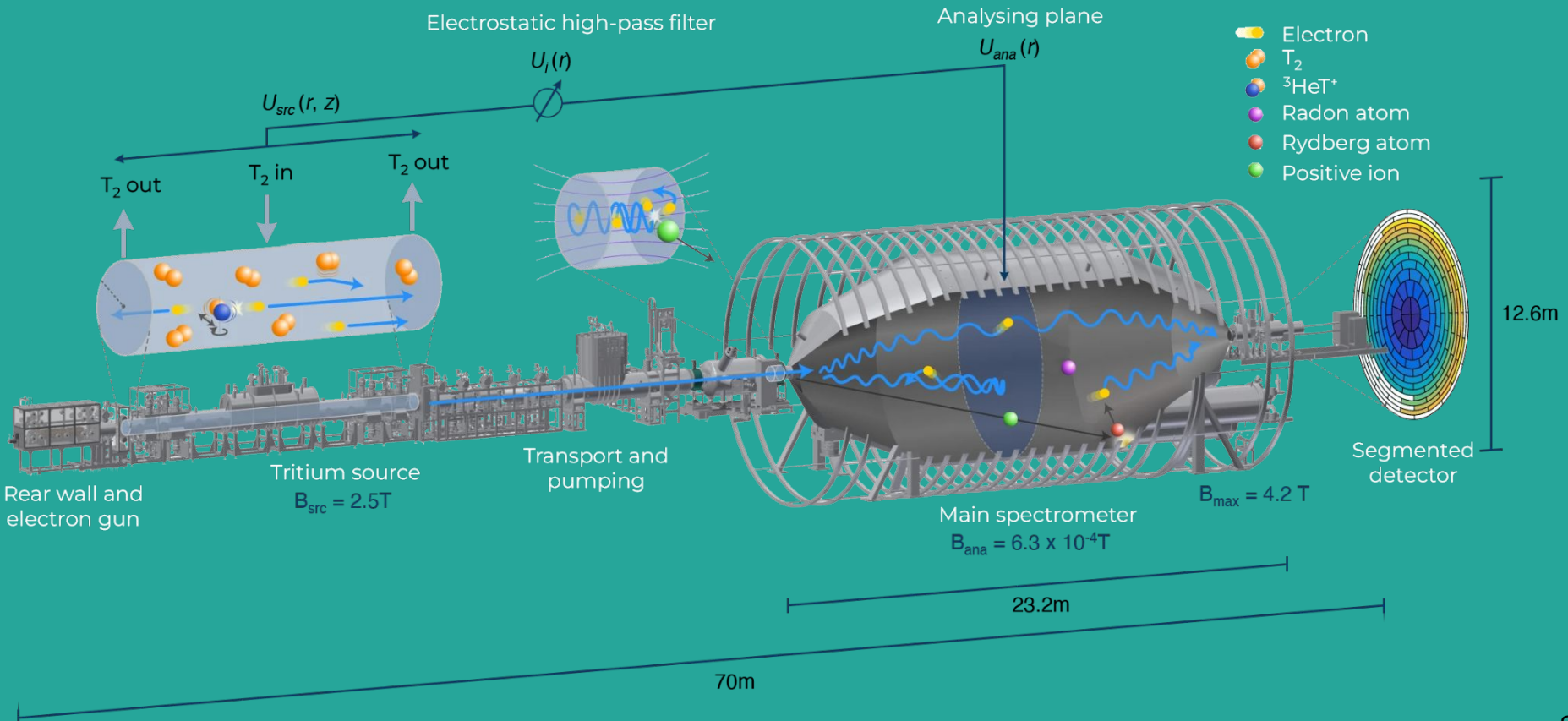
we can model the effective decay rate $R_\beta(E_e; m_{\nu_e}^2)$ for a given radioactive element: **Tritium!**

Recipe for the most precise ever ν_e mass measurement

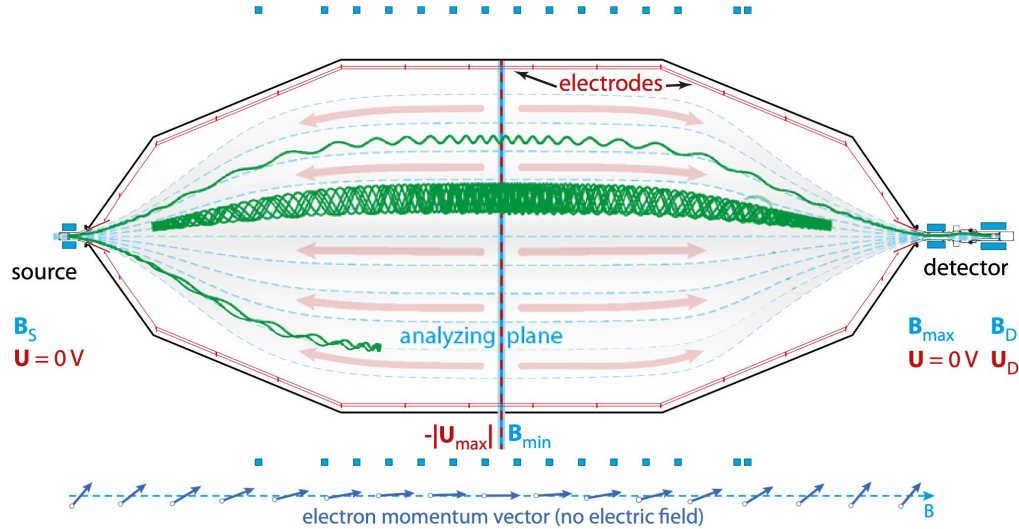
- A highly stable β^- radiation source \Rightarrow Tritium decay!
- A super precise energy filter for the β^- electrons
- A very tightly controlled environment for the e^- , to suppress backgrounds as much as possible

The KATRIN Experiment

The KATRIN Experiment



MAC-E Spectrometer



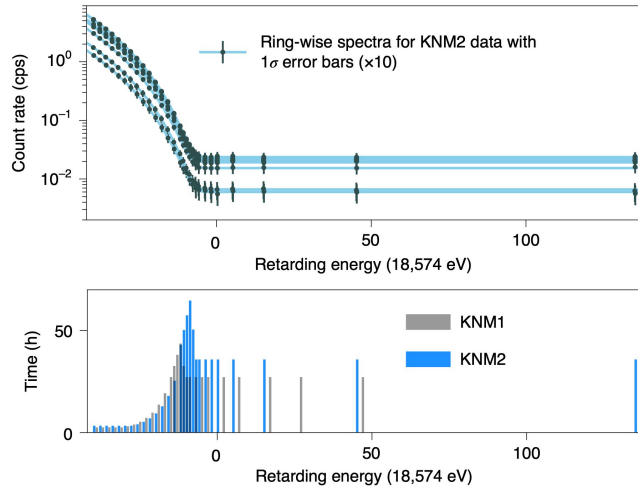
$$\frac{p_{\perp}^2}{B_{\min}} = \text{const}$$

- ❑ 24 superconducting magnets
- ❑ **Adiabatic high-pass filter (no energy change)**
- ❑ Wide electron angular acceptance

$$\theta_{\max} = \arcsin \sqrt{\frac{B_{\text{src}}}{B_{\max}}} = 50.4^{\circ}$$

$$\Delta E = 18.6 \text{ keV} \times \frac{B_{\min}}{B_{\max}} = 2.8 \text{ eV}$$

Measurement



- Detector divided in **12 rings**
- **Measurement Time varies for each energy configuration (scan step)**, to reduce statistical uncertainty

$$E_0 - 300 \text{ eV} \leq qU_i \leq E_0 + 135 \text{ eV}$$

The KATRIN Modelling

Modelling

The model constructed to fit the data has two major components:

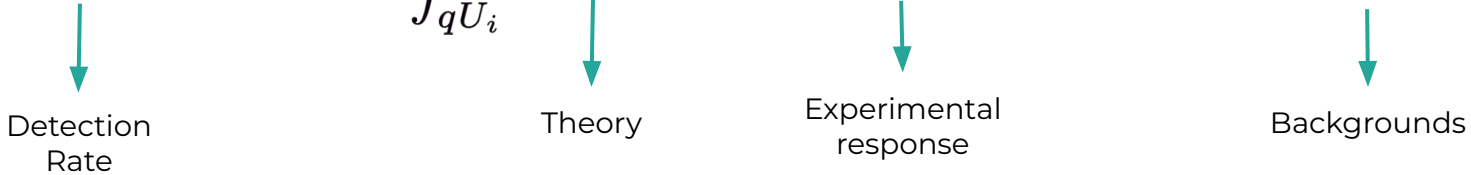
1. The **theory**
2. The **response function**



Modelling

The model constructed to fit the data has two major components:

1. The **theory** (β -decay spectrum given by Fermi's theory)
2. The **response function** = Experiment (Hardware)

$$R(qU_i, r_j) = A_s^j N_T \int_{qU_i}^{E_0^j} R_\beta(E; m_\nu^2) f(E, qU_i, r_j) dE + R_{\text{bg}}(qU_i, r_j).$$


Detection Rate

Theory

Experimental response

Backgrounds

⇒ It makes possible to **compare the data and the simulations.**

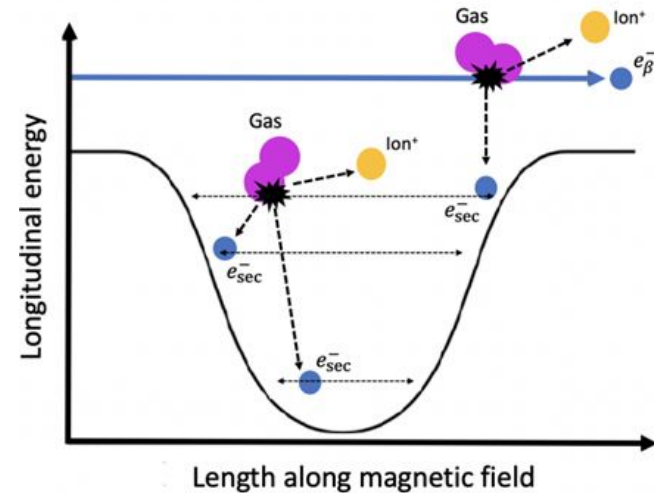
How can
KATRIN
experiment
measure m_ν
precisely?



Background Description

Main sources of background

- **Radioactive decays:** ^{210}Po , ^{219}Rn and ^{220}Rn
(Present on the **surface of the spectrometer**)
- **Penning trap**
 - Electrons trapped **between the two spectrometers** can create an **avalanche**
 - Electron catchers installed to **“clean”** the trap **between scan steps**



Systematic Uncertainties

Breakdown of uncertainties

Effect	68.2% CL uncertainty on m_ν^2 (eV ²)
Statistical	0.29
Non-Poissonian background	0.11
Source-potential variations	0.09
Scan-step-duration-dependent background	0.07
qU -dependent background	0.06
Magnetic fields	0.04
Molecular final-state distribution	0.02
Column density \times inelastic scattering cross section	0.01
Activity fluctuations	0.01
Energy-loss function	<0.01
Detector efficiency	<0.01
Theoretical corrections	<0.01
High-voltage stability and reproducibility	<0.01
Total uncertainty	0.34

The uncertainties of the individual systematic effects are quoted in the main text.

Statistics is the main source of uncertainty

Discussed on next slides:

- 1. Background related**
- 2. Source-potential variations**

Background mis-modelling

Modelled using simulation

- Non-Poissonian but Gaussian
- Width only 11% larger

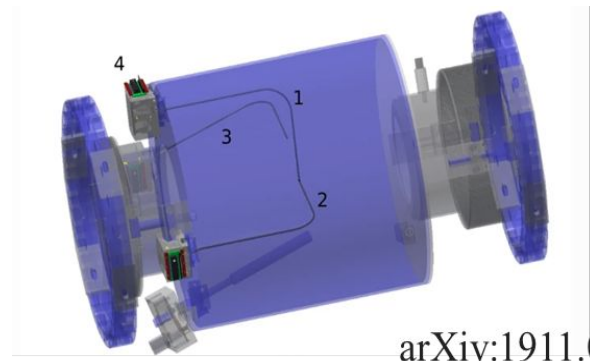
Electron catcher *only between scan steps*

- Linear term for (small) accumulation
- Reference measurement constraints slope of term

Retardation potential dependence

- Background can **depend on potential**
- Linear term, constraint from dedicated measurement

Effect	68.2% CL uncertainty on m_ν^2 (eV ²)
Statistical	0.29
Non-Poissonian background	0.11
Source-potential variations	0.09
Scan-step-duration-dependent background	0.07
qU -dependent background	0.06



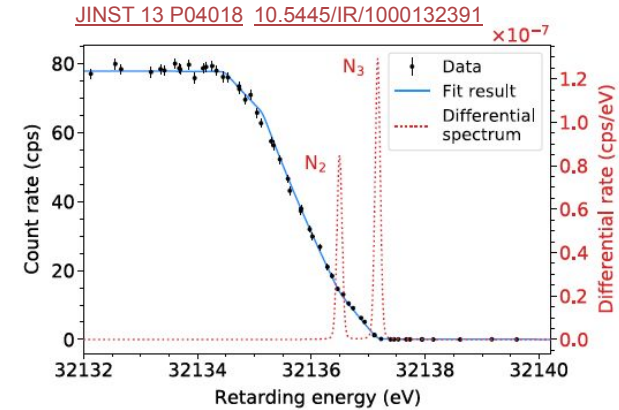
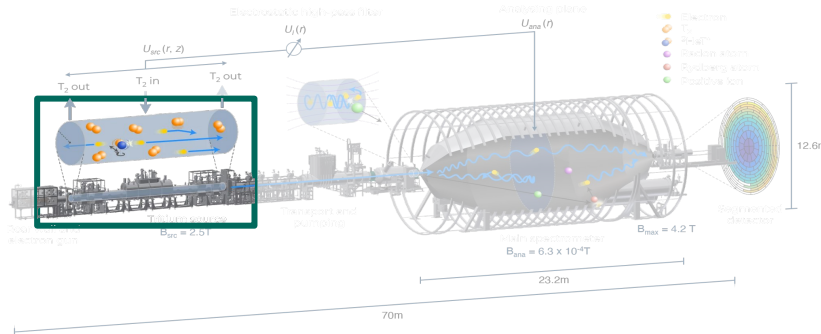
arXiv:1911.09633

Source Potential Variations

→ Potential variations can cause spectral distortions

- Asymmetry **shifts electron spectrum** of scattered vs unscattered
- **Assess variation with ^{83m}Kr spectroscopy** by co-circulating gas
 - Broadening of electron conversion lines (N2 and N3) reveals information about the potential variations
- Approximately **Gaussian** with width 61 MeV

Effect	68.2% CL uncertainty on m_e^2 (eV ²)
Statistical	0.29
Non-Poissonian background	0.11
Source-potential variations	0.09
Scan-step-duration-dependent background	0.07
qU -dependent background	0.06



Neutrino Mass Inference

Neutrino Mass Inference

⇒ Inference of m_ν^2 **by fitting** the experimental spectrum with prediction by minimizing:

$$\chi^2 = (\mathbf{R}_{\text{data}}(q\mathbf{U}, \mathbf{r}) - \mathbf{R}(q\mathbf{U}, \mathbf{r} \mid \Theta, \eta))^T \cdot C^{-1} (\mathbf{R}_{\text{data}}(q\mathbf{U}, \mathbf{r}) - \mathbf{R}(q\mathbf{U}, \mathbf{r} \mid \Theta, \eta))$$

Θ : Free parameters

- **Most important parameter: m_ν^2**
- **12 ring-dependent parameters**

⇒ $1 + (3 \times 12) = 37$ parameters

η : additional nuisance parameters

Neutrino Mass Inference

4 independent methods used

- **Pull Method:**

$$\chi_{\text{tot}}^2(\Theta, \eta) = \chi^2(\Theta, \eta) + \sum_i \left(\frac{\hat{\eta}_i - \eta_i}{\sigma_{\eta_i}} \right)^2$$

- **Covariance matrix method:** covariance matrix from $O(10^4)$ beta-decay spectrum simulations
- **Monte Carlo propagation method:** fit repeated 10^5 times, systematic parameters varied according to PDF, fit parameter distributions extracted
- **Bayesian Inference:** flat and positive \mathbf{m}_ν^2 prior

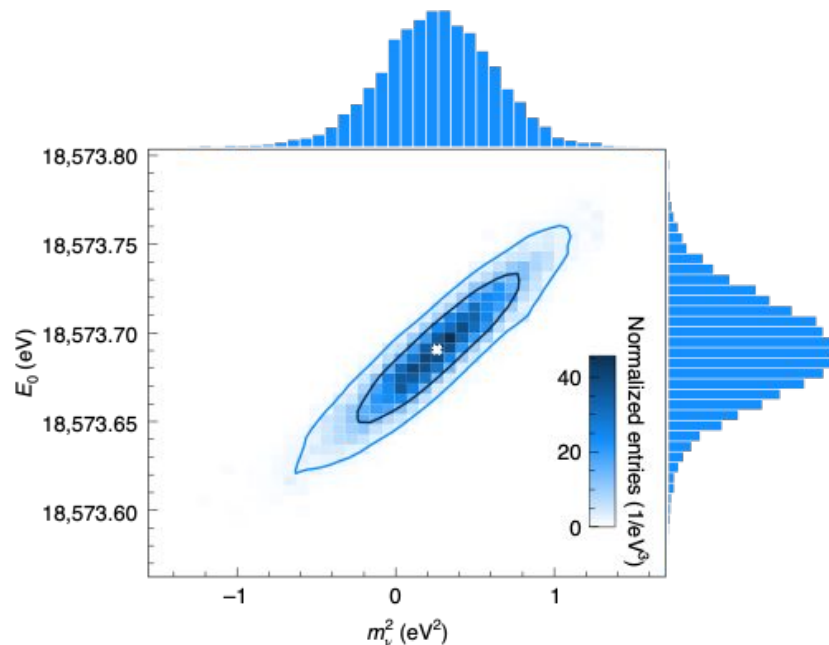
Neutrino Mass Inference

- **Best fit** (MC propagation method)

$$m_\nu^2 = 0.26 \pm 0.34 \text{ eV}^2$$

- The independent analyses **agree** within about **5% of the total uncertainty**
- **Limit setting**: 3 methods (2 frequentist, 1 Bayesian) at 90% C.L.

$$m_\nu < 0.9 \text{ eV}$$

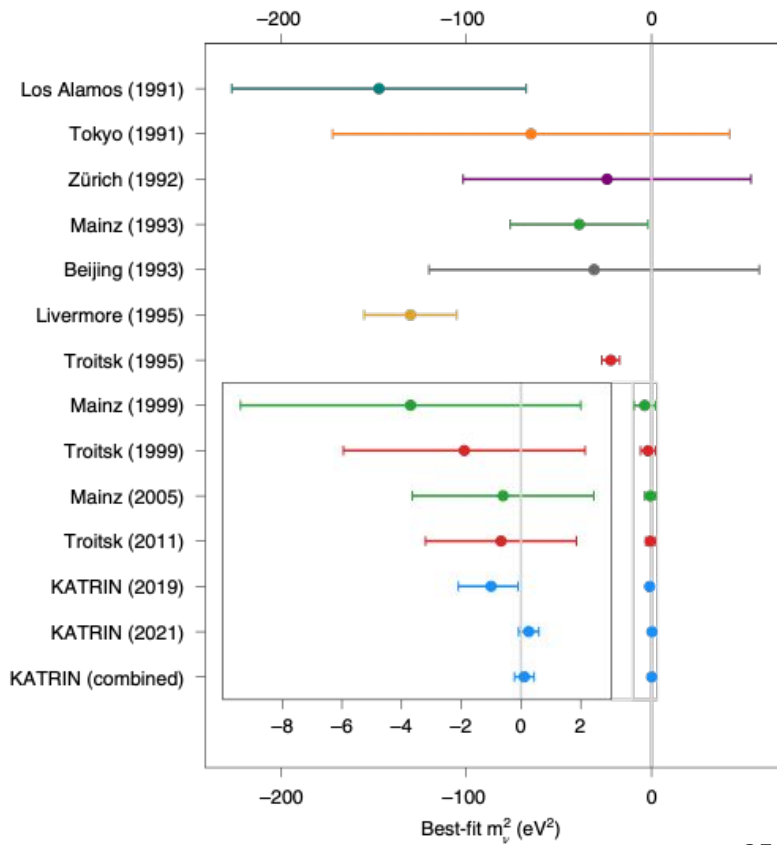


Conclusions and prospects

- **Combining** this best fit with previous KATRIN results:

$$m_\nu < 0.8 \text{ eV}$$

- **First sub-eV measurement!**
- **The goal:** Reduce the upper limit to $\sim 0.2 \text{ eV}$ by both **taking more data** and **modelling systematics** better.

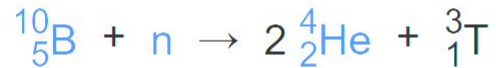
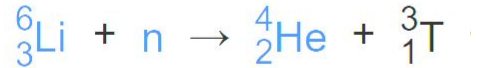


Backup

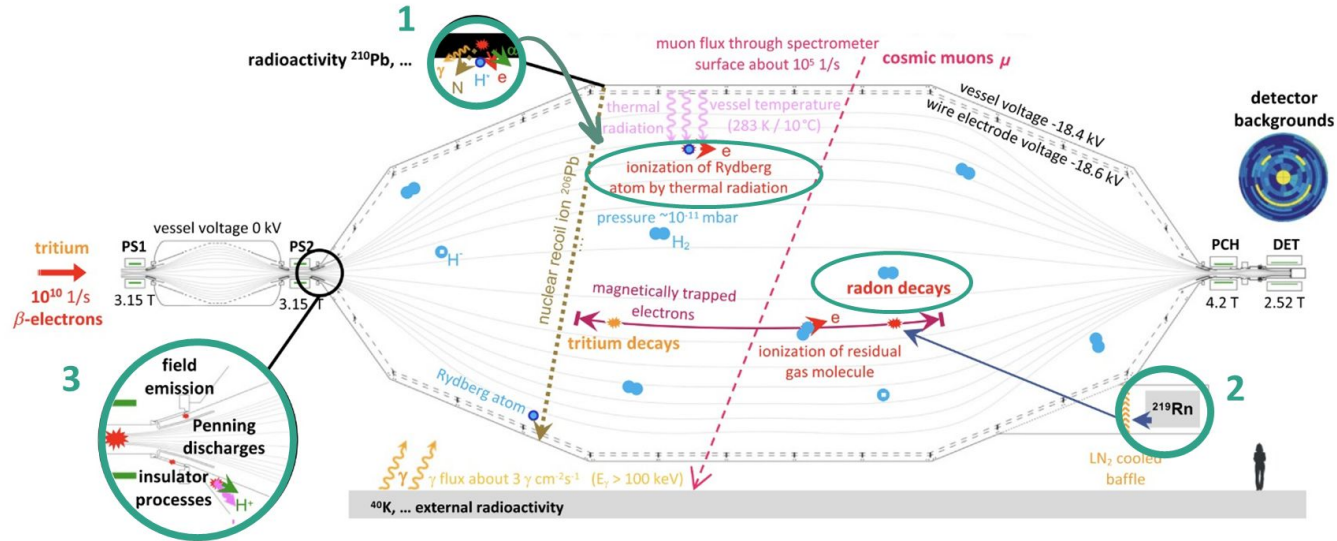


How is Tritium produced

- Naturally occurring tritium is extremely rare, and must be synthetically produced
- Lithium-6, Lithium-7 and Boron-10 produce tritium via nuclear fission originated by neutron activation



Main sources of background

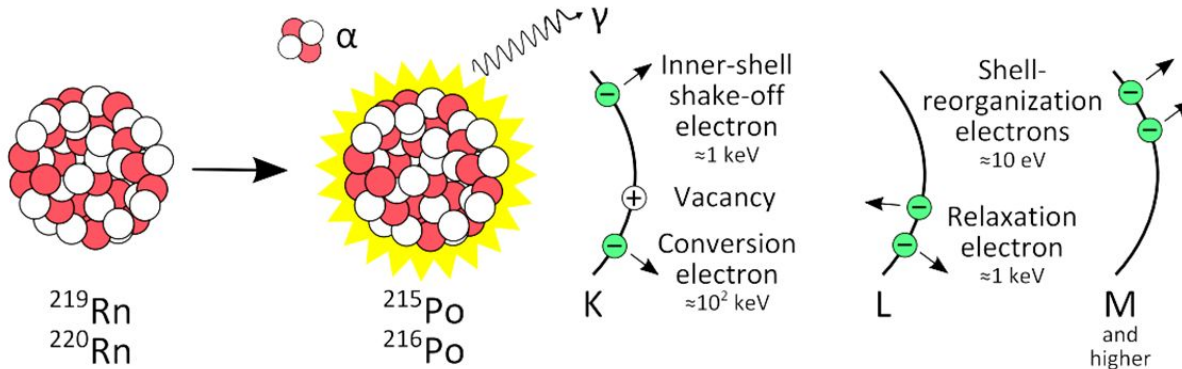


1. Recoiling Pb-206 coming from alpha decays of Po-210 create highly excited Rydberg states
2. Decays of Rn-219(220) into Po-215(216) and subsequent emission of electrons that slowly cool down by ionizing residual gas in the spectrometer
3. Ions created in Penning trap between the pre and main spectrometer

Among others (e.g. muons from cosmic rays, ...)

Main sources of background

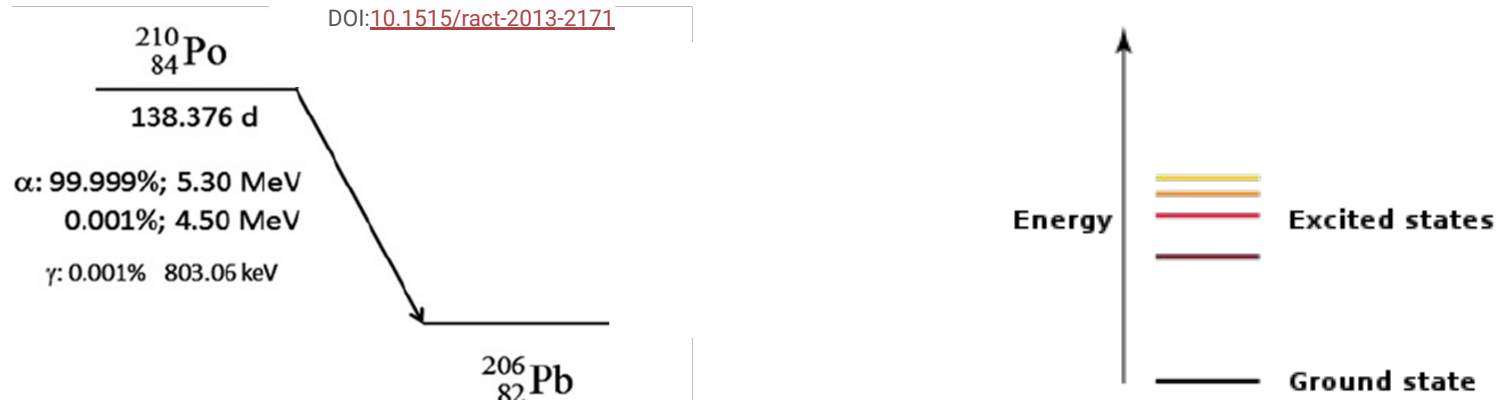
Decays of $^{219(220)}\text{Rn}$ into $^{215(216)}\text{Po}$ and subsequent emission of e^-



- Dominant source of systematic uncertainty
- Non-Poissonian background coming from Radon decays inside the volume of the spectrometer into excited states of Polonium, that subsequently emits electrons
- The resulting low-energy electrons are accelerated by retarding energy qU_{ana} towards the focal-plane detector, making them indistinguishable from signal electrons using the energy information only

Main sources of background

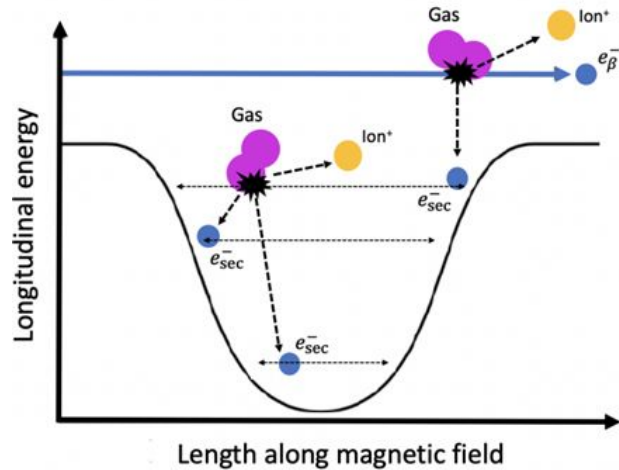
Recoiling ^{206}Pb coming from α decays of ^{210}Po create highly excited Rydberg states



- Arising from α -decays of ^{210}Po in the structural material of the spectrometer
- The recoiling ^{206}Pb creates highly electronically excited Rydberg states at the inner spectrometer surfaces, which can be ionized during propagation in the inner volume by thermal radiation.
- Resulting low-energy electrons are accelerated by retarding energy qU_{ana} towards the focal-plane detector, making them indistinguishable from signal electrons using the energy information only.

Main sources of background

Ions created in a Penning trap between the pre and main spectrometer

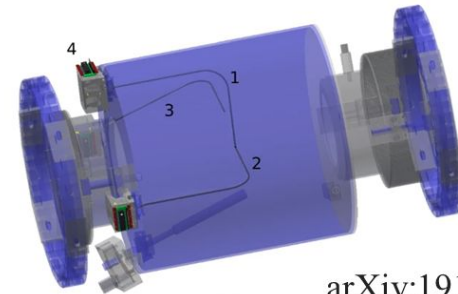


- Residual gas is ionized, an ion and secondary electron is created.
- Low energy secondary electrons are trapped in the potential well and ionize in turn residual gas molecules.
- e⁻ accumulating in the Penning can lead to elevated background rates

An exponentially growing avalanche or discharge may present a danger for the spectrometer and detector section of KATRIN

To counteract this problem, “electron catchers” (1-3) were installed in the beamline inside the magnet bore between the two spectrometers

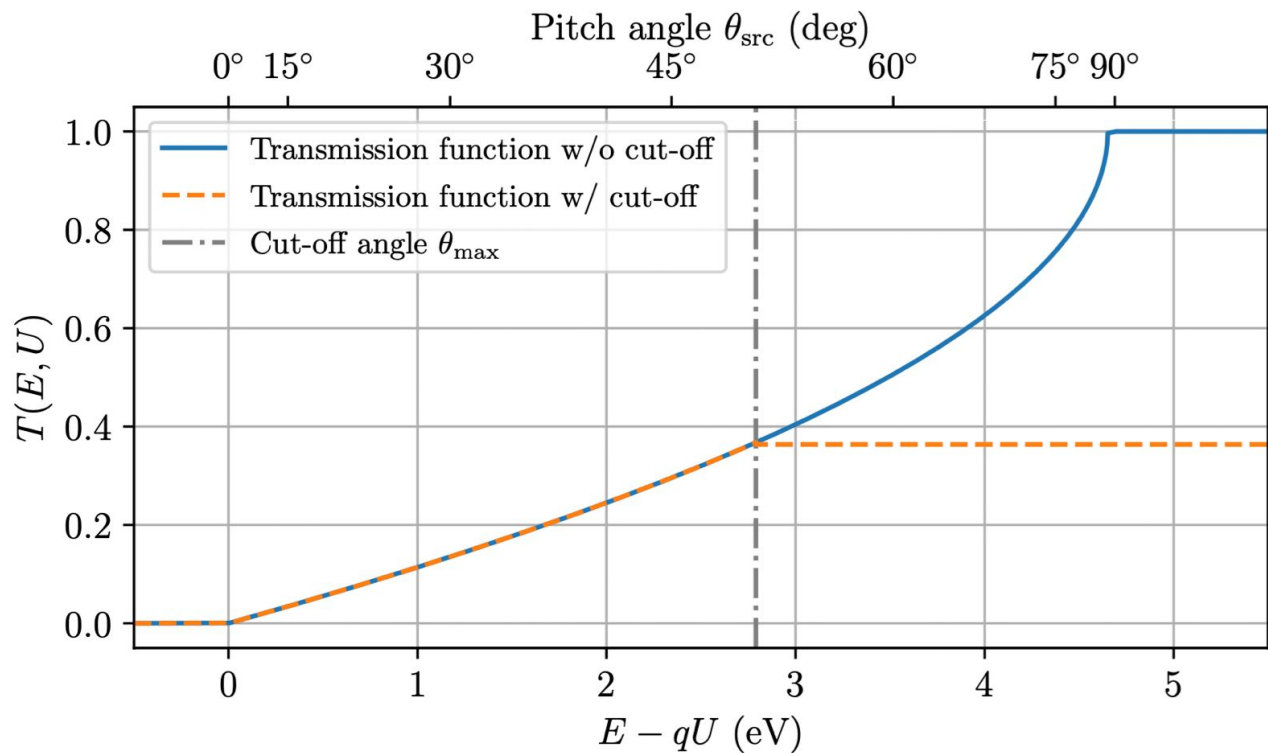
pre-spectrometer side main spectrometer side



arXiv:1911.09633

The trap is emptied after each scan step

Transmission Function



Source Potential Variations

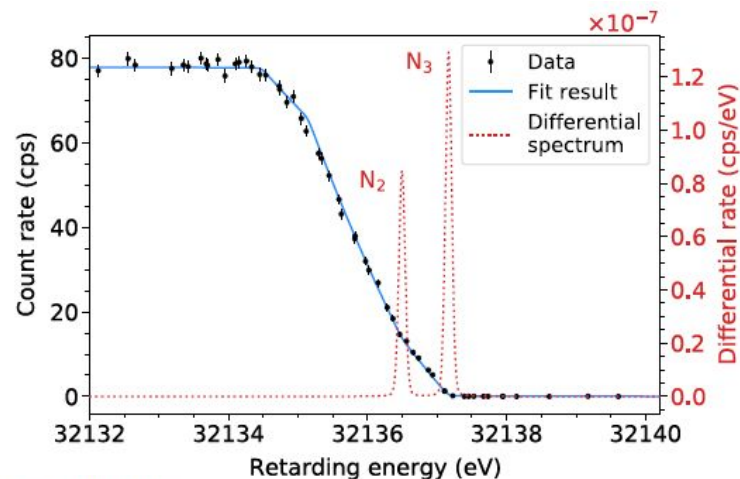
JINST 13 P04018
 10.5445/IR/1000132391

Variations on the potential can lead to spectral distortions. This asymmetry of the potential results in a shift in the energy spectrum associated with the scattered electrons compared with the spectrum of the unscattered

$$f(E - qU) = \int_{\epsilon=0}^{E-qU} \int_{\theta=0}^{\theta_{\max}} \mathcal{T}(E - \epsilon, \theta, U) \sin \theta \cdot \sum_s P_s(\theta) f_s(\epsilon) d\theta d\epsilon$$

energy-loss function $f_{s=1}(\epsilon)$ of singly scattered ($s=1$) electrons is shifted by Δ_p relative to the energy-loss function $f_{s=0}(\epsilon)$ of unscattered ($s=0$) electrons.

Both parameters are assessed with the help of co-circulating ^{83m}Kr gas, assuming that the possible plasma instabilities or longitudinal plasma profile are not affected by its presence in a minute concentration. The spectroscopy of its mono-energetic conversion electron lines reveals information about the broadening σ_p of the lineshape, from which an upper limit of Δ_p is derived⁸². from a uniform distribution in the range of $-\sigma_p/1.3 \leq \Delta_p \leq \sigma_p/1.3$. The resulting distribution can be approximated by a Gaussian distribution centred around 0 meV with a width of 61 meV.



Extended Data Fig. 2 | Measurement of the internal conversion lines (N_2/N_3) of ^{83m}Kr . This exemplary measurement was performed at 40 % of the nominal column density. The black data points show the measured rate with statistical uncertainty for each retarding energy. The fit to the data (blue line) infers the broadening σ_p^2 (40%). Details can be found in the section **Source Potential Calibration** in the Methods part. The visible width of the measured spectrum is dominated by the energy resolution of the spectrometer. The red dotted line illustrates the underlying differential spectrum of the N_2/N_3 doublet, broadened by the fitted σ_p^2 value. The red y-axis corresponds to the differential spectrum.

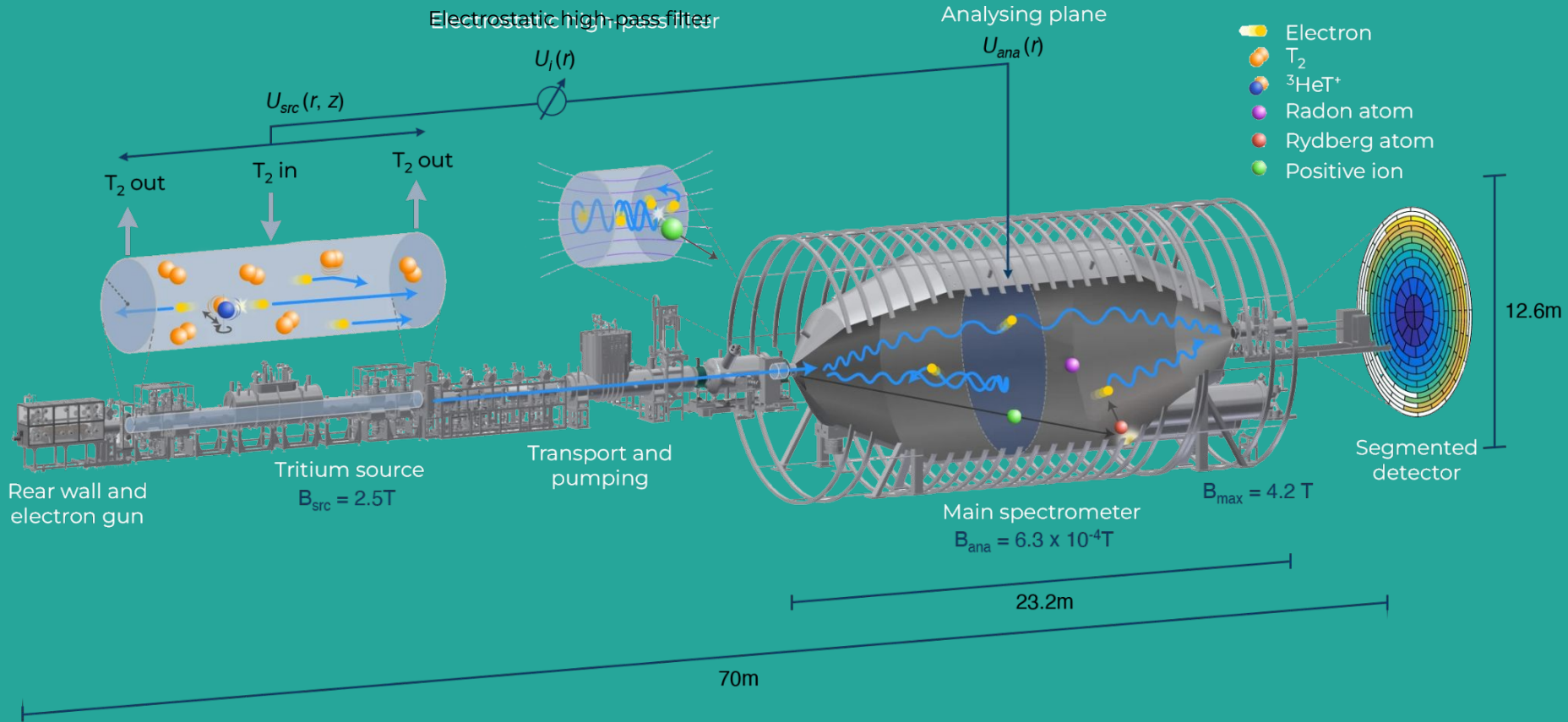
Doppler Broadening (backup slide)

The Doppler broadening of the spectral energies is an unpleasant circumstance in precision spectroscopy. This is caused by the random motion of the gas molecules.

The source gas is cooled to 30 K to reduce thermal motion of tritium molecules; This also allows a greater density of molecules in the source container.

The differential beta-emission spectrum ($R_\beta(E)$) includes radiative corrections and the molecular final-state distribution;

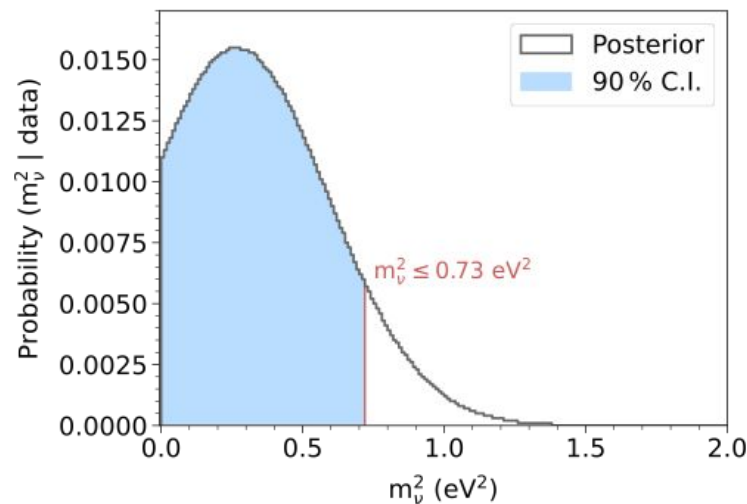
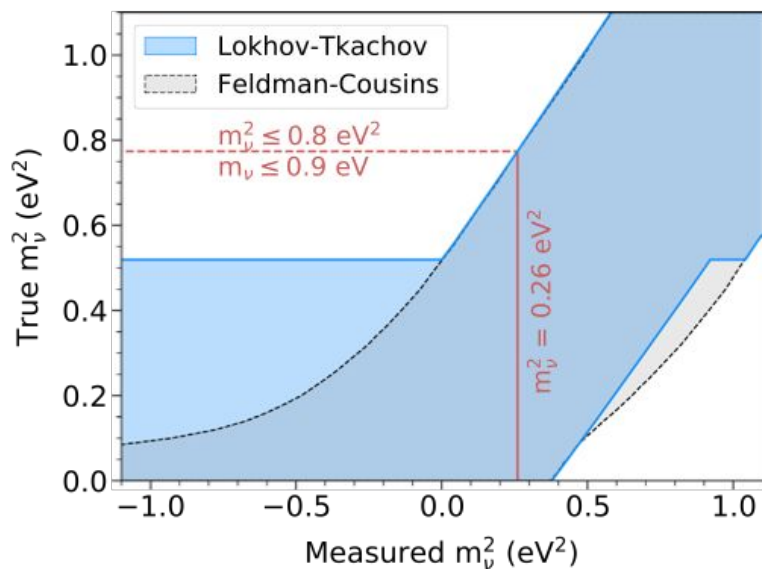
The final-state distribution uses a gaussian broadening to emulate the doppler broadening (due to the thermal motion of the molecules) as well as energy broadenings due to spatial and temporal variations in the spectrometer and source electric potential.



Neutrino Mass Inference

⇒ Defining the upper limit

The χ^2 minimization reveals an excellent goodness of fit with a χ^2 per degree of freedom of 0.9, corresponding to a p value of 0.8.



Feldman-Cousins confidence intervals (frequentist)

- Feldman-Cousins introduces a new ordering principle based on the likelihood ratio:

$$R = \frac{P(x|\mu)}{P(x|\mu_{best})}$$

Here x is the measured value, μ is the true value, and μ_{best} is the best fit (maximum likelihood) value of the parameter given the data and the physical allowed region for μ .

- The order procedure for fixed μ is to add values of x to the interval from highest R to lower R until you reach the total probability content you desire.
- Taking a ratio “renormalizes” the probability when the measured value is unlikely for any value of μ . The Feldman-Cousins confidence interval is therefore never empty.

Lokhov-Tkachov confidence intervals (frequentist)

The random variable θ is a function of a set of experimental data X . We define $L_\alpha(\theta)$ and $U_{\alpha'}(\theta)$ as:

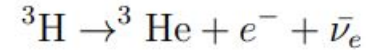
$$P(-\infty < \hat{\theta} < L_\alpha(\theta)) = \alpha, \quad P(U_{\alpha'}(\theta) < \hat{\theta} < +\infty) = \alpha'.$$

And define the confidence level β :

$$P(L_\alpha(\theta) < \hat{\theta} < U_{\alpha'}(\theta)) = 1 - \alpha - \alpha' \equiv \beta$$

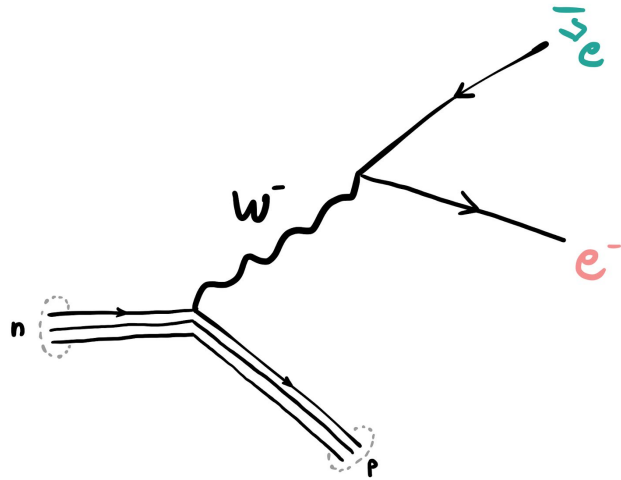
Note that the curve $\theta = u(\hat{\theta})$ cannot exceed $\theta = u_{1-\beta}(\hat{\theta})$. Any such a pair of curves forms what will call *allowed confidence belt* for the confidence level β .

Future developments



- KATRIN aims to have sensibility of 0.2 eV at 90% CL
- Must have even lower systematics and background rate
- Current bkg: 220 mcps (10⁻³ counts per second)
- Need: 10 mcps

We can produce ν_e through the β^- decay, and ...



we can model the effective decay rate $R_\beta(E_e; m_{\nu_e}^2)$ for a given radioactive element